High Accuracy In-Flight Wavelength Calibration of Imaging Spectrometry Data

Alexander F.H. Goetz[1,2], Kathleen B. Heidebrecht[1] and Thomas G. Chrien[3]

[1]Center for the Study of Earth from Space/CIRFiS, University of Colorado
[2]Department of Geological Sciences, University of Colorado
[3]Jet Propulsion Laboratory, California Institute of Technology

1. INTRODUCTION

Accurate wavelength calibration of imaging spectrometer data is essential if proper atmospheric transmission corrections arc to be made to obtain apparent surface reflectance (Gao et al., 1993). Accuracies of 0,1 nm arc necessary for a 10 nm-sampling instrument in order to match the slopes of the deep atmospheric water vapor features that dominate the 0.7-2.3 μm region(Goetz et al., 1991).

AVIRIS (Vane et al., 1993) is calibrated in the laboratory to determine the wavelength position and full-width-half-maximum (FWHM) response for each of the 224 channels (Chrien et al., 1990). The accuracies arc limited by the quality of the monochromator used as a source. The accuracies vary from iO.5 to ±1.5 nm depending on the wavelength region, in general decreasing with increasing wavelength. Green et al. (1990; 1992) make corrections to the wavelength calibrations by using the known positions of 14 atmospheric absorption features throughout the 0.4-2.5pm wavelength region. These features, having varying width and intensity, were matched to the MODTRAN model (Berk et al., 1989) with a non-linear least squares fitting algorithm. A complete calibration was developed for all 224 channels by interpolation.

instrument calibration cannot bc assumed to bo stable to 0.1 nm over a flight season given the rigors of thermal cycling and launch and landing loads, The upcoming sensor HYDICE (Rickard et al., 1993) will require a mums for in-flight spectral calibration of each scene because the calibration is both temperature and pressure sensitive. In addition, any sensor using a two-dimensional army has the potential for systematic wavelength shifts as a function of cross-track position, commonly called "smile" (Goetz et al., 1991). Therefore, a rapid means for calibrating complete images will bc required. The following describes a method for determining instrument wavelength calibration using atmospheric absorption features that is efficient enough to bc used for entire images on workstations. This study shows the effect of the surface reflectance on the calibration accuracy and the calibration history for the AVIRIS B spectrometer over the 1992 flight season.

2. METHOD

The O_2 absorption feature, centered at 762 nm, was used here to test various methods for instrument calibration, The data used came from eight flights spanning the 1992 flight season for AVIRIS. Since only the 762 nm band was used, only the B spectrometer calibration of AVIRIS was tested.

The standard models, such as ATREM (Gao c; al., 1993), used for radiometric correction arc based on spectral atmospheric transmission values given in HITRAN (Rothman et al., 1987). In ATREM the HITRAN data arc resampled to provide an equal wavelength spacing of 2.5 nm. Therefore, wc chose to represent the 02 feature with 2,5 nm samples, deemed adequate given the AVIRIS FWHM of 9 nrn and sampling of approximately 10 nm (fig. 1). Three AVIRIS channels arc affected by the 02 band, but

the shape of the band is dependent on the wavelength position of each individual detector (fig, 2).

The apparent shape of the O_2 band is dependent not only on the individual detector wavelength and spectrometer resolution, but also on the shape of the spectral reflectance curve within the three channels affected (fig 3). This effect has been recognized by others (Gao and Goetz, 1990; Carrere and Conel, 1993) and accounted for in the non-linear least squares fitting routines. However, non-linear least squares is a computing intensive technique, not suitable for processing large image data sets rapidly.

The method chosen here makes usc of the slopes of the spectral curves about the band-center wavelength channel (fig 4). The model spectrum is resampled using 100 different sets of wavelengths, each differing by 0.1nm. Ratios of slope(left)/slope(right) arc taken and the results for all possible ratios arc shown in figure 5. The procedure for determining the actual wavelength of the center channel is as follows: (1) Divide the AVIRIS radiance spectrum by the cxo-atmospheric solar irradiancc spectrum. (2) Correct for the slope of the surface spectral reflectance by assuming a linear change in reflectance between the channels adjacent to the channels affected by the 02 absorption. (3) Calculate the ratio of the slopes of the two sides of the 02 feature. (4) Determine the center wavelength from the look-up table, the values of which arc plotted in figure 5.

3. RESULTS

Figure 6 shows the results of an analysis of a full scene of data from the June 21, 1992 coverage of Blackhawk Island, Wisconsin. The histograms show the distribution of calculated ccntcr-channel wavelength values for data with and without surface reflectance corrections. The separation between the two peaks is the greatest for vegetated areas because the 762 nm band lies at the shoulder of the NIR plateau in vegetation reflectance. The width of the distributions can bc attributed to system noise and variations in surface materials. Therefore, it is important to calculate the band center for a large number of pixels to get an accurate wavelength value. Figure 7 shows the results calculated from vegetated and unvegetated areas within the Blackhawk island image. The offset between the two curves is.4 nm and can bc attributed to the assumption of a linear surface reflectance curve over the 50 nm wavelength region bridging the 02 absorption feature. and the width of the distribution can bc attributed to system noise only,

A number of images from the 1992 AVIRIS flight season were processed. The center wavelength position was constant for scenes from two different overflights taken on the same day. Figure 8 shows the variation of the center wavelength position of channel 42 with time. The wavelength calibration file accompanying the image data gives a value of 764.0 nm. The maximum variation is only 3 nm, but this becomes significant when atmospheric correction is attempted. Figure 9 shows the results of the application of the ATREM program to data from Gainesville, Florida taken July 8 under very high humidity conditions. The proper calibration is most important here because of the great depth of the unsaturated atmospheric water absorption features. The properly calibrated data set has far fewer artifacts than the onc using the published wavelength values. AVIRIS contains an onboard calibration capability using filters. The data have not yet been checked to confirm the shift.

4. CONCLUSIONS

Wc have shown that, at least for the 762 nm 02 absorption band, it is possible to calibrate AVIRIS , using in-flight data, to an accuracy of ±0.2 nm regardless of the surface reflectance. This technique could bc extended to other atmospheric features in the wavelength range covered by AVIRIS and HYDICE. The rapid analysis made possible by our algorithm will make it feasible to analyze each image from sensors such as HYDICE, for which systematic wavelength calibration changes during flight arc

anticipated.

5. ACKNOWLEDGMENT

The authors wish to thank Bruce Kindel of CSES for AVIRIS image analysis. This research was supported by NASA GSFC under contract no. NAS5-317 11.

6. REFERENCES

Berk, A., 1..S. Bernstein and D.C. Robertson, 1989, "MODTRAN: a moderate resolution model for LOWTRAN 7," Air Force Geophysical Laboratory, Hascomb AFB, MA. 42.

Carrere, V. and J.E. Conel, 1993, "Recovery of Atmospheric Water Vapor Total Column Abundance from Imaging Spectrometer Data around 940 nm - Sensitivity Analysis and Application to Airborne Visible/lnfrarcd Imaging Spectrometer (AVIRIS) Data," *Remote Sens. Environ. , vol.* 44, no. 2/3, pp. 179-204.

Chrien, 'J'.G., R.O. Green and M.L. Eastwood, 1990, *Accuracy of the Spectral and Radiometric Laboratory Cailbtation of the Airborne Visible/Infrared imaging Spectrometer (AVIRIS),* Second Airborne Visible/Infrared Imaging Spectrometer (AVIRIS) Workshop, Pasadena, CA, NASA, pp. 1-14.

Gao, B.-C. and A.F.H. Goetz, 1990, "Column Atmospheric Water Vapor and Vegetation Liquid Water Retrievals From Airborne Imaging Spectrometer Data," *J. Geophys. Res. , vol. 95,* no. D4, pp. 3549-3564.

Gao, B.-C., K, Il. Heidebrecht and A.F.H. Goetz, 1993, "Derivation of Scaled Surface Reflectances from AVIRIS Data," *Remote Sens. Environ. , vol. 44,* no. 2/3, pp. 165-178.

Goetz, A. F.H., C.O. Davis, J.D. Aber, K.L. Carder, R.N. Clark, J. Dozier, S.A.W. Gerstl, H. Kieffer, D.A. Landgrebe, J.M. Melack, L.C. Rowan, S.L. Ustin, R.M. Welch and C.A. Wessman, 1991, "nigh Resolution Imaging Spectrometer (HIRIS) Science Requirements," HIRIS Science Team and Jet Propulsion 1 aboratory. 30.

Green, R. O., J.E. Conel, C.J. Bruegge, J.S. Margolis, V. Carrere, G. Vane and G. Hoover, 1992, ***In-flight calibration*** *of* ***the spectral and radometric characteristics*** *of AVIRIS in 1991,* Third Annual JPL Airborne Geoscience Workshop, Pasadena, CA, JPL, pp. 1-4.

Green, R.O., J.E. Conel, V. Carrère and c. al., 1990, *Determination of the in-flight spectral and radiometric characteristics of the Airborne Visible/Infrared Imaging Spectrometer (A VIRIS),* Second AVIRIS Workshop, Pasadena, CA, JPL, pp. 15-22.

Rickard, I.. J., R.W. Basedow, E.F. Zalewski, P.R. Silverglate and M. Landers, 1993, *HYDICE: an airborne system for hyperspectral imaging,* SPIE - Imaging Spectrometry of the Terrestrial Environment, Orlando, FL, SPIE, pp. 173-179.

Rothman, 1.. ., R.R. Gamache, A. Goldman, L.R. Brown, R.A. Toth, H.M. Pickett, R.L. Poynter, J.-M. Flaud, C. Camy-peyret, A. Barbe, N. Husson, C.P. Rinsland and M. A. H. Smith, 1987, "The HITRAN database: 1986 edition," *Appl. Opt* , vol. 26, no. pp. 4058-4097.

Vane, G., R.O. Green, T.G. Chrien, H.T. Enmark, E.G. Hansen and W.M. Porter, 1993, "The Airbomc Visible/Infrared Imaging Spectrometer," *Remote Sens. Environ. , vol. 44,* no. 2/3, pp. 127-143.

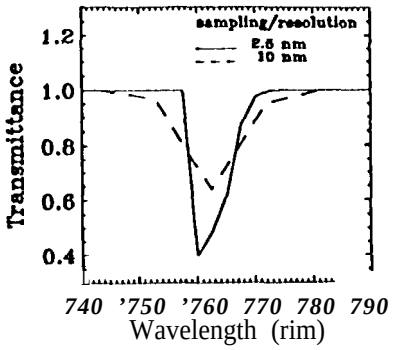

Figure 1. The oxygen feature at HITRAN and AVIRIS resolution and sampling,

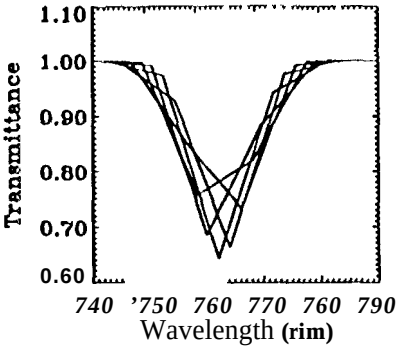

Figure 2. Oxygen band with sensor center wavelengths varying by 2 nm.

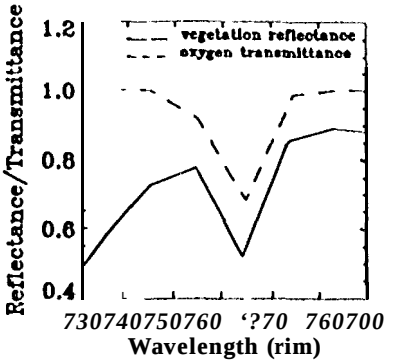

Figure 3. Oxygen transmittance and vegetation reflectance spectra. Note the increasing s1ow in the vegetation spectrum.

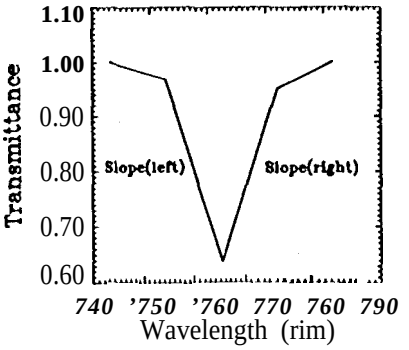

Figure 4. The left and right sides of the oxygen feature are used in calculating the ratio.

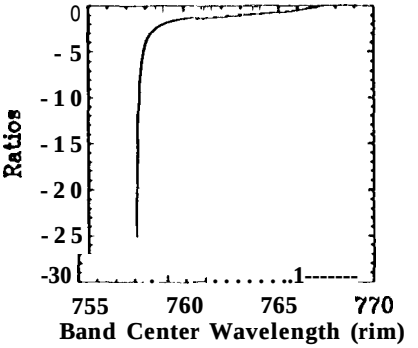

Figure 5. Ratios of two sides of the oxygen feature for 100 different sensor wavelength calibrations.

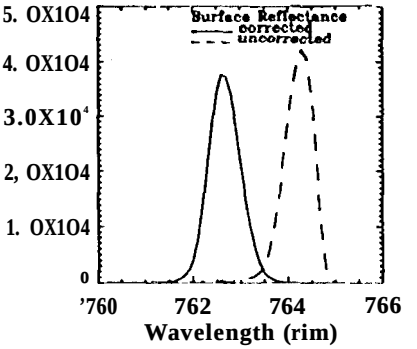

Figure 6. Oxygen band center histograms for the full Blackhawk Island scene, corrected and uncorrected for surface reflectance.

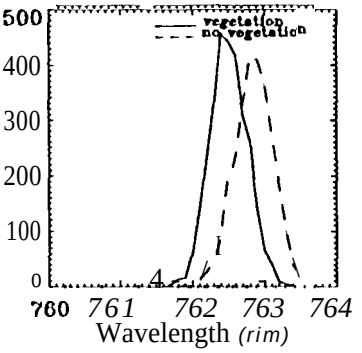

Figure 7. Histograms of the oxygen band centers for vegetated and nonvegetated areas near Blackhawk Island.

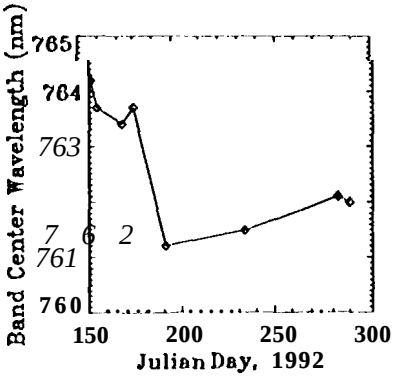

Figure 8. Calculated oxygen band center wavelengths for eight scenes over the 1992 flight season.

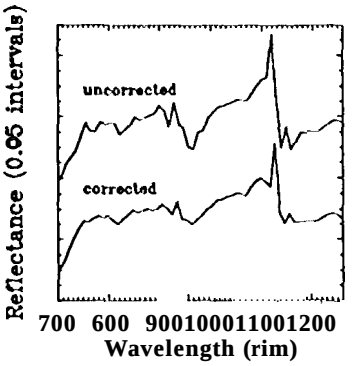

Figure 9. Reflectance spectra in AVIRIS spectrometer B calculated using ATREM from Gainesville, Florida. Wavelengths for the corrected spectrum were shifted by 2.8 nm.